

Short communication

Novel thixotropic gel electrolytes based on dicationic bis-imidazolium salts for quasi-solid-state dye-sensitized solar cells

Jun Young Kim^{a,b}, Tae Ho Kim^{a,*}, Dong Young Kim^c,
Nam-Gyu Park^c, Kwang-Duk Ahn^{b,**}

^a Department of Polymer Science and Engineering, SungKyunKwan University, Suwon, Kyunggi-do 440-746, Republic of Korea

^b Functional Polymer Lab., Korea Institute of Science and Technology, Seoul 136-791, Republic of Korea

^c Energy Materials Research Center, Korea Institute of Science and Technology, Seoul 136-791, Republic of Korea

Received 5 June 2007; received in revised form 9 August 2007; accepted 20 August 2007

Available online 4 September 2007

Abstract

Novel thixotropic gel electrolytes have been successfully prepared by utilizing oligomeric poly(ethylene oxide) (PEO)-based bis-imidazolium diiodide salts and hydrophilic silica nanoparticles for application in quasi-solid-state dye-sensitized solar cells (DSSCs). The thixotropic gel-state of the ionic liquid-based composite electrolytes is confirmed by observing the typical hysteresis loop and temporary hydrogen bonding. On using the PEO-based composite electrolyte, a quasi-solid-state DSSC exhibited highly improved properties such as easy penetration of the electrolyte into the cell without leakage, long-term stability, high open-circuit voltage without the use of 4-*tert*-butylpyridine, and a high energy-conversion efficiency of 5.25% under AM 1.5 illumination (100 mW cm⁻²).

© 2007 Elsevier B.V. All rights reserved.

Keywords: Poly(ethylene oxide)-based bis-imidazolium salts; Gel electrolyte; Thixotropic gel; Quasi-solid-state dye-sensitized solar cell; Energy-conversion efficiency

1. Introduction

The first report on a new type of dye-sensitized solar cell (DSSC) was published by Grätzel and co-worker [1] and, by improving TiO₂ electrodes they attained an overall energy conversion efficiency of 10% in simulated solar light [2,3]. Since then, DSSCs have been intensively studied and have attracted an ever-growing interest from many researchers of different disciplines. DSSCs based on mesoporous TiO₂ nanocrystals are attractive candidates for a new renewable energy resources because they can be made with low-cost materials through a simple manufacturing process [4–7]. Nevertheless, there are many issues that need to be resolved for DSSCs achieve practicality such as increasing the conversion efficiency and achieving better long-term stability.

The photovoltaic effect in a DSSC originates from the interface between a redox electrolyte containing iodide and triiodide (I⁻/I₃⁻) ions and a ruthenium dye-adsorbed mesoscopic TiO₂ electrode [8]. The electrolyte, as one of the key ingredients, provides internal electric conductivity by diffusing within the mesoporous TiO₂ layer [9]. Because of their relatively high ionic conductivity and low viscosity, room-temperature ionic liquids (RTIL) are being widely investigated as solvents and important sources for the iodide-based redox couple in DSSCs [10–12]. To prevent the leakage of RTIL-based electrolytes, quasi-solid-state electrolytes have been proposed by incorporating low-molecular weight gelating agents [13–16] and the addition of fumed silica nanoparticles [17–19]. Grätzel et al. [20] reported that ionic, liquid-based, composite electrolytes were successfully employed for a quasi-solid-state DSSC system that gave 7% conversion efficiency at AM 1.5 illumination. The reported composite electrolyte was found, however, to be incomplete in the formation of gel-state because it consisted of 1-methyl-3-propylimidazolium iodide as a low-viscosity ionic liquid and fumed silica nanoparticles with low specific-surface areas. Recently, Yang et al. [21] have reported the formation of

* Corresponding author. Tel.: +82 31 290 7281; fax: +82 31 292 8790.

** Corresponding author. Tel.: +82 2 958 5281; fax: +82 2 958 5308.

E-mail addresses: kimth@skku.edu (T.H. Kim), kdahn@kist.re.kr (K.-D. Ahn).

a solid-state electrolyte by using 1-butyl-3-methylimidazolium salt with a different anion, such as tetrafluoroborate, and fumed silica nanoparticles. The electrolytes they reported were solid-state and showed only a melting behaviour and they did not explain changes in viscosity like the thixotropic gel-state.

Thixotropic gels can be converted into sols by applying a suitable mechanical stress, e.g., by shaking, and then the sols return to gels again at a definite rate when the stress is removed. The advantage of thixotropic gel electrolytes is that it can easily penetrate the mesoporous TiO₂ layer by shearing (sol-state), and thereby provide enhanced dye-adsorbed TiO₂/electrolyte interfacial contact. The open-circuit voltage (V_{oc}) of a DSSC is significantly influenced by surface treatment with pyridine derivatives such as, *N*-methylbenzimidazole, tetrabutylammonium phosphate, and recently with guanidinium derivatives [22,23]. In particular, the addition of 4-*tert*-butylpyridine (tBP) to the redox electrolyte gives a significant improvement in the V_{oc} [24]. This was attributed to the masking of electrons at the TiO₂ surface.

In this work, novel thixotropic gel electrolytes are prepared by employing dicationic bis-imidazolium diiodide salts (PEO_{*m*}BIm-I) and hydrophilic fumed silica to improve both the solidification tendency of an electrolyte system and the V_{oc} without using tBP in DSSCs. To the best of our knowledge, this is the first report of the use of thixotropic gel electrolytes based on imidazolium salts as ionic liquids for DSSCs.

2. Experimental

2.1. Synthesis of PEO-based dicationic bis-imidazolium diiodide salts

Three kinds of PEO_{*m*}BIm-I salts (where *m* is the number of ethylene oxide (EO) units of PEO) were prepared and are based on PEO oligomers that have two *N*-butylimidazolium cations on the both chain ends. The salts have a structure of two butylimidazolium dications formed by joining different EO linkages, as described in Scheme 1. α,ω -Dichloro substitution reactions were carried out with poly(ethylene glycol) (average molecular weight 100, 300, and 600) and SOCl₂. The procedure was based on the earlier published work of Johansson et al. [25]. The α,ω -dichloro-PEO oligomers (average EO units of 2, 6, 13) were then reacted with an excess of 1-butylimidazole at 80 °C for 3 days to obtain PEO_{*m*}BIm-Cl with a yield of 90%. The chloride anions of PEO_{*m*}BIm-Cl were replaced by iodide anions via an ion-exchange reaction with sodium iodide in ultra-low water acetonitrile (water contents: 10 ppm) at 40 °C for 12 h to obtain PEO_{*m*}BIm-I. The reaction mixture was filtered through

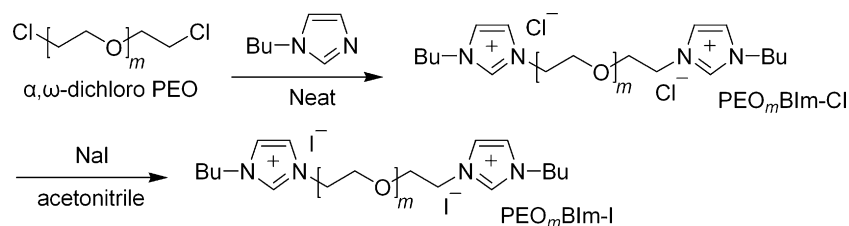
a Celite® 545 layer to remove sodium salts and then poured into dehydrated diethylether. The resulting viscous precipitate was collected and then dried in vacuum at 80 °C for 2 days. The structures of these PEO derivatives were confirmed by ¹H NMR spectroscopy, i.e., PEO₂BIm-I: yield 96%, T_g -51 °C, T_d 240 °C, ¹H NMR (DMSO-*d*₆, δ) 0.883 (t, 6H, J =7.3 Hz, CH₃-butyl), 1.202–1.264 (m, 4H, CH₂-butyl), 1.733–1.782 (m, 4H, CH₂-butyl), 3.520 (s, 4H, OCH₂CH₂O), 3.742 (t, 4H, J =4.8 Hz, NCH₂-CH₂-O), 4.190 (t, 4H, J =7.2 Hz, NCH₂-butyl), 4.332 (t, 4H, J =4.8 Hz, NCH₂-CH₂-O), 7.740–7.810 (d, 4H, Imz-C(4,5)H), 9.168 (s, 2H, Imz-C(2)H). PEO₆BIm-I: yield 89%, T_g -51 °C, T_d 230 °C, ¹H NMR (DMSO-*d*₆, δ) 0.886 (t, 6H, J =7.2 Hz, CH₃-butyl), 1.233–1.423 (m, 4H, CH₂-butyl), 1.815–1.967 (m, 4H, CH₂-butyl), 3.556 (s, 4H, OCH₂CH₂O), 3.813 (t, 4H, J =4.4 Hz, NCH₂-CH₂-O), 4.210 (t, 4H, J =7.2 Hz, NCH₂-butyl), 4.352 (t, 4H, J =4.4 Hz, NCH₂-CH₂-O), 7.750–7.840 (d, 4H, Imz-C(4,5)H), 9.188 (s, 2H, Imz-C(2)H). PEO₁₃BIm-I: yield 80%, T_g -49 °C, T_d 239 °C, ¹H NMR (CDCl₃, δ) 0.892 (t, 6H, J =7.4 Hz, CH₃-butyl), 1.266–1.461 (m, 4H, CH₂-butyl), 1.813–1.965 (m, 4H, CH₂-butyl), 3.605 (s, 4H, OCH₂CH₂O), 3.920 (t, 4H, J =4.4 Hz, NCH₂-CH₂-O), 4.245 (t, 4H, J =7.2 Hz, NCH₂-butyl), 4.405 (t, 4H, J =4.2 Hz, NCH₂-CH₂-O), 7.755–7.846 (d, 4H, Imz-C(4,5)H), 9.748 (s, 2H, Imz-C(2)H).

2.2. Preparation of electrolytes

The reference liquid electrolyte was composed of 0.6 M 1-hexyl-2,3-dimethylimidazolium iodide, 0.1 M lithium iodide (LiI), 0.05 M iodide (I₂), and 0.5 M tBP in 3-methoxypropionitrile (MPN). In order to investigate the photocurrent density–voltage (J - V) characteristics of the PEO_{*m*}BIm-I with different EO units as the iodide source, three types of PEO_{*m*}BIm-I-based liquid electrolytes (PEO_{*m*}BIm-I/MPN, volume ratio=1:1) were prepared. The liquid electrolytes were: 0.25 M I₂ in PEO₂BIm-I/MPN, 0.15 M I₂ in PEO₆BIm-I/MPN, and 0.15 M I₂ in PEO₁₃BIm-I/MPN. An amount (5 wt.%) of hydrophilic fumed silica nanoparticles (Aerosil 300, 7 nm primary particle size, Degussa) was mixed by means of a bead shaker (MS1 Minishaker, IKA with zirconia bead) in the PEO₁₃BIm-I-based liquid electrolytes to form thixotropic gel electrolytes.

2.3. Preparation of electrodes and cell assembly

The nanocrystalline TiO₂ electrode was fabricated by depositing TiO₂ colloidal paste (Ti-Nanoxide D, Solaronix SA) on fluorine-doped SnO₂ conducting glass (FTO, TEC 8,



Scheme 1.

sheet resistance of $8\text{--}10\ \Omega\ \text{cm}^{-2}$, Pilkington) using a simple doctor-blade technique. The layer was dried in the air at room temperature for 30 min and sintered at $500\ ^\circ\text{C}$ for 30 min to obtain a mesoporous TiO_2 film that had a thickness of about $11\ \mu\text{m}$. After being sintered, the TiO_2 electrodes were cooled down to $80\ ^\circ\text{C}$ and dye-coated by immersing them into a $0.4\ \text{mM}$ solution of an amphiphilic dye (Ruthenium 535-bisTBA, Solaronix SA as referred to N-719) in absolute ethanol at room temperature for 20 h. The dye coating was done immediately after high temperature annealing in order to avoid rehydration of the TiO_2 surface or capillary condensation of water vapour from ambient air inside the mesopores of the film. The dye-anchored electrode was then rinsed with ultra-low water acetonitrile and dried in a stream of argon. The Pt counter electrodes were prepared by coating H_2PtCl_6 solution ($7\ \text{mM}$ in isopropyl alcohol) on to the FTO and then sintering at $450\ ^\circ\text{C}$ for 15 min. The electrodes were separated by a $25\ \mu\text{m}$ -thick thermoplast hot-melt sealing film (SX1170-25, Solaronix SA) as a spacer and sealed by heat. The liquid or thixotropic gel electrolyte was introduced into the interelectrode space from the Pt counter electrode side through a pre-drilled hole. The hole was sealed with a microscope cover slide using SX1170 hot-melt to avoid leakage of the electrolyte.

2.4. Instruments and measurement

^1H NMR spectra of the $\text{PEO}_m\text{BIm-I}$ salts were taken on a Varian INOVA 600 ($600\ \text{MHz}$) FT-NMR using tetramethylsilane as an internal standard. IR spectra were recorded on a Perkin-Elmer Spectrum GX1 ATR FT-IR spectrophotometer. Thermal analysis was carried by differential scanning calorimetry (DSC) Q100 with a refrigerated cooling system and a 2950HR AutoTGA instrument (TA Instruments) at a heating rate of $10\ ^\circ\text{C}\ \text{min}^{-1}$ under a nitrogen atmosphere. Thixotropic behaviour or shear measurements were performed on a programmable cone/plate-type viscometer (spindle CPE-41, HBDV-II+, Brookfield Engineering Lab.) using a thermostated water bath. An electronic gap setting system was

also used for all measurements. Cell performance was evaluated using an AM 1.5 solar simulator (Oriel 91193 with a $1\ \text{kW}$ ozone-free Xenon source as an irradiation source). The active area of the TiO_2 electrode was $0.150\ \text{cm}^2$ and the incident light intensity was adjusted with a NREL-calibrated Si solar cell (PV Measurements Inc.) for 1 SUN ($100\ \text{mW}\ \text{cm}^{-2}$) intensity. The $J\text{--}V$ curves were measured at AM 1.5 illumination using a Keithley Model 2400 unit. Each value for cell performance was taken as the average of 10 samples.

3. Results and Discussion

3.1. Formation of $\text{PEO}_m\text{BIm-I}$ -based gel

The hydrophilic fumed silica nanoparticles (Aerosil 300) were added as a gelating agent at $5\ \text{wt.}\%$ to solidify the $\text{PEO}_m\text{BIm-I/MPN}$ ($1:1\ \text{v/v}$) solutions. Among the various mixtures of $\text{PEO}_m\text{BIm-I/MPN}$ and hydrophilic silica nanoparticles, the gelation was only detected for the $\text{PEO}_{13}\text{BIm-I}$, as shown in Fig. 1. In particular, the $\text{PEO}_{13}\text{BIm-I}$ -based silica composite electrolyte clearly exhibits gel formation, as shown in Fig. 1(e). The composite electrolyte goes into a gel-state by adding Aerosil 300 nanoparticles to the $\text{PEO}_{13}\text{BIm-I}$ -based liquid electrolyte at more than $4\ \text{wt.}\%$. However, no gelation is observed in the mixture of $\text{PEO}_{13}\text{BIm-I}$ and hydrophobic fumed silica nanoparticles (Aerosil R812, after treated with hexamethyldisiloxane based on Aerosil 300, Degussa) even though the weight portions of Aerosil R812 nanoparticles are $5\text{--}10\ \text{wt.}\%$, as shown in Fig. 1(d). These results suggest that temporary three-dimensional hydrogen bonds between the silanol groups on the surface of hydrophilic silica nanoparticles and the PEO chain in $\text{PEO}_{13}\text{BIm-I}$ are produced to form the gel-state, thereby preventing the flow of the resulting mixture. To understand the mechanism of the gelation, the FT-IR spectra of a mixture of $\text{PEO}_{13}\text{BIm-I/MPN}$ and Aerosil 300 nanoparticles were compared with those of a mixture of $\text{PEO}_{13}\text{BIm-I/MPN}$ and Aerosil R812 nanoparticles, as shown in Fig. 2. In the Aerosil 300 nanoparticles mixed with a $\text{PEO}_{13}\text{BIm-I/MPN}$ solution, the

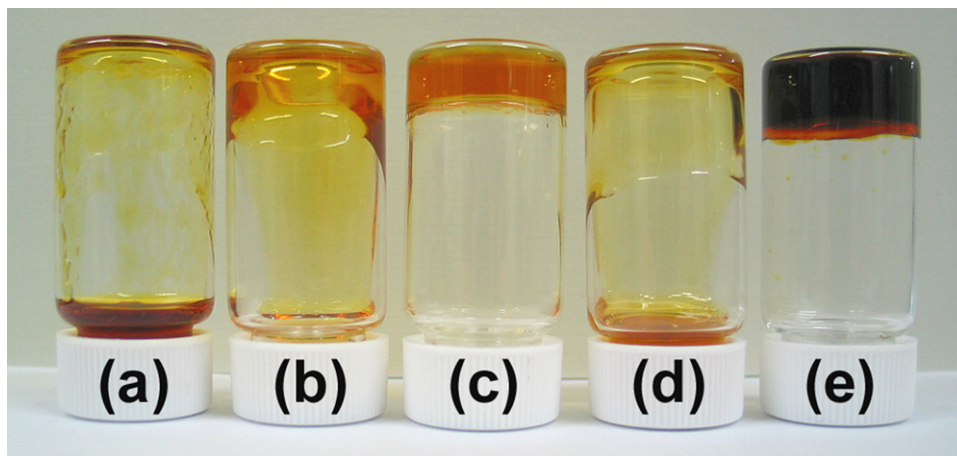


Fig. 1. Photographs of the mixtures of $\text{PEO}_m\text{BIm-I/MPN}$ ($1:1\ \text{v/v}$) and silica nanoparticles ($5\ \text{wt.}\%$) in a bottle by turning upside down. (a) $\text{PEO}_2\text{BIm-I/MPN/Aerosil 300}$, (b) $\text{PEO}_6\text{BIm-I/MPN/Aerosil 300}$, (c) $\text{PEO}_{13}\text{BIm-I/MPN/Aerosil 300}$, (d) $\text{PEO}_{13}\text{BIm-I/MPN/Aerosil R812}$ and (e) thixotropic gel electrolyte ($0.15\ \text{M}\ \text{I}_2$ in mixture (c)).

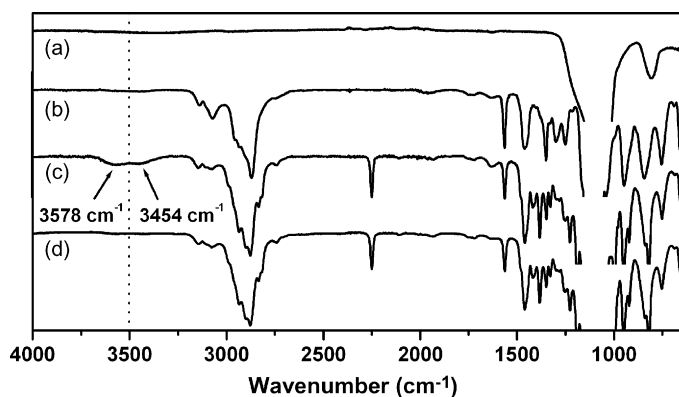


Fig. 2. FT-IR spectra of PEO₁₃BIm-I/MPN-based gel. (a) Aerosil 300, (b) PEO₁₃BIm-I, (c) PEO₁₃BIm-I/MPN/Aerosil 300 (5 wt.%) and (d) PEO₁₃BIm-I/MPN/Aerosil R812 (5 wt.%).

broad vibration bands appear at 3578 and 3454 cm⁻¹, indicating obvious interaction of the PEO chain in PEO₁₃BIm-I with silanol groups. By contrast, no appreciable change in the FT-IR spectrum of the PEO₁₃BIm-I/MPN/Aerosil R812 system is observed. Therefore, the gelation originates from hydrogen bonds between the silanol groups of Aerosil 300 nanoparticles and the polyether chain in PEO₁₃BIm-I.

3.2. Thixotropic behaviours

The thixotropic loop of the PEO₁₃BIm-I/MPN/Aerosil 300 system in Fig. 3(a) shows an upward line (filled circle) and a downward line (open circle) depending on an increase and a decrease in the shear rate, respectively. The shear rate in Fig. 3(a) increases from 0.27 to 2.69 s⁻¹ within 20 s and remains at a constant value of 2.69 s⁻¹ for 5 s, and then decreases from 2.69 to 0.27 s⁻¹ within 40 s. The evolution of viscosity as a function of shear rate results from the hysteresis loop. The presence of a hysteresis area in Fig. 3(a) indicates that the PEO₁₃BIm-I/MPN/Aerosil 300 system exhibits time-dependent rheological behaviour, i.e., thixotropy. The shear stress curve confirms shear thinning behaviour since the shear stress decreases at a constant rate, as shown in Fig. 3(b). This thixotropic behaviour of the PEO₁₃BIm-I-based gel electrolyte is maintained over many weeks in the same sample bottle after taking away aliquot portions many times. By changing the gel to the sol state, the PEO₁₃BIm-I-based thixotropic gel electrolyte can readily penetrate into the TiO₂ mesopores, resulting in better interfacial contact.

3.3. Photovoltaic properties of quasi-solid-state DSSCs

Typical *J*-*V* characteristics for cells with the PEO_{*m*}BIm-I-based liquid electrolytes having different EO units without using tBP at 1 SUN intensity are presented in Table 1. By increasing the PEO length of the PEO_{*m*}BIm-I, the *V*_{oc} values are significantly improved when the PEO_{*m*}BIm-I-based liquid electrolyte is injected into the dye-anchored TiO₂, since the longer PEO chain can be easily adsorbed on to the surface of TiO₂. This finding is consistent with the hypothesis reported by Komiya et

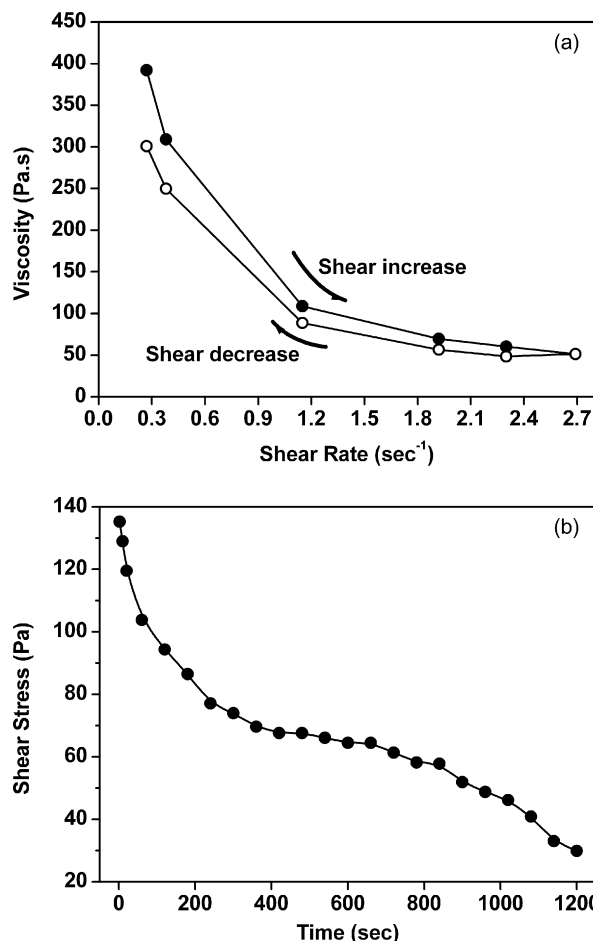


Fig. 3. (a) Hysteresis loop and (b) shear stress as function of time for mixture, PEO₁₃BIm-I/MPN/Aerosil 300 (5 wt.%) at constant shear rate of 2.69 s⁻¹ for 20 min by a Brookfield HBDV-II+ cone/plate viscometer at 25 ± 0.1 °C.

al. [26]. The decrease in *V*_{oc} is known to be caused by a back electron transfer reaction in which I₃⁻ is reduced to I⁻ by taking an electron from the TiO₂ conduction band. The PEO₁₃BIm-I adsorbed on the TiO₂ surface suppresses the back electron transfer from the TiO₂ to the I₃⁻ in the electrolyte, thereby causing a higher value of *V*_{oc}.

The photovoltaic performance of a quasi-solid-state DSSC with a PEO₁₃BIm-I-based thixotropic gel electrolyte at different light intensities is given in Fig. 4 and listed in Table 2. By increasing the light intensity of simulated AM 1.5 solar irradiation, the values of *V*_{oc}, short-circuit current density (*J*_{sc}) and conversion efficiency (*η*) are increased. The *V*_{oc} increases with light intensity, while the value of fill factor (FF) decreases due to ohmic losses in the conducting glass. In the case of low light

Table 1
Comparison of *J*-*V* characteristics for DSSC with PEO_{*m*}BIm-I-based liquid electrolytes (PEO_{*m*}BIm-I/MPN, volume ratio = 1:1) without using tBP

Iodide source	Iodine concentration (M)	<i>V</i> _{oc} (mV)	<i>J</i> _{sc} (mA cm ⁻²)	FF	<i>η</i> (%)
PEO ₂ BIm-I	0.25	617	11.23	0.67	4.63
PEO ₆ BIm-I	0.15	683	12.10	0.66	5.46
PEO ₁₃ BIm-I	0.15	730	11.61	0.66	5.60

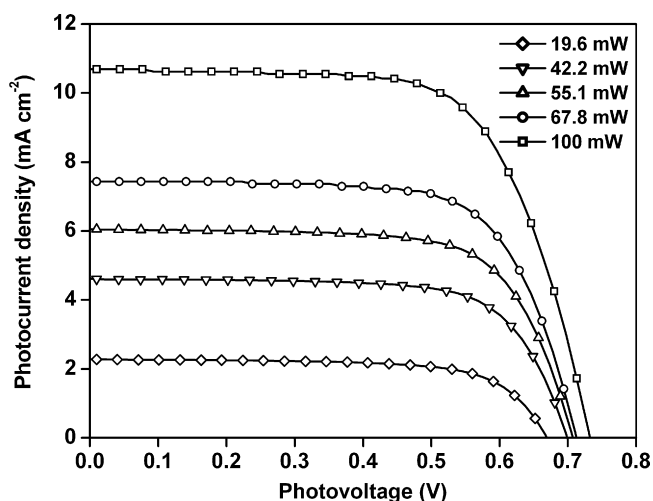


Fig. 4. Photocurrent density–voltage curves of DSSCs with PEO₁₃BIm-I-based thixotropic gel electrolyte: measured at different light intensities; TiO₂ layer thickness of 11 μm .

intensity, the small amount of the excited state of the dye in the working electrode causes a low value of J_{sc} , whereas the small amount of oxidized dye and iodide in the system give rise to a low concentration of triiodide and results in a low value of V_{oc} . With increase in light intensity, the amount of excited state of dye increases and thereby the increases the V_{oc} and the J_{sc} , respectively. Interestingly, the conversion efficiency is not reduced at an irradiation of 1 SUN. This suggests that the transport ability of iodide or triiodide ions in the thixotropic gel electrolyte is not limited to a high light intensity.

The J_{sc} values of the thixotropic gel electrolyte increase linearly with light intensity up to 1 SUN, as shown in Fig. 5. This linearity indicates that the photocurrent is not limited by diffusion of iodide or triiodide ions within the TiO₂ electrode. To compare the thixotropic gel electrolyte performance with the reference liquid electrolyte in DSSC systems, the J – V characteristics were measured, the results are presented in Fig. 6. A quasi-solid-state DSSC using a PEO₁₃BIm-I-based thixotropic gel electrolyte (shown in Fig. 1(e)) exhibits a conversion efficiency of 5.25% without using tBP. A quasi-solid cell with a PEO₁₃BIm-I-based thixotropic gel electrolyte has a comparable V_{oc} value to that of the reference liquid electrolyte containing tBP. The low J_{sc} value of PEO₁₃BIm-I-based electrolyte is considered to be due to the retarded mobility of triiodide ions in the redox media. The long-term stability of the quasi-solid-state DSSCs using a PEO₁₃BIm-I-based thixotropic gel electrolyte is also maintained without extra sealing for over 6 months. The

Table 2

Parameters of photovoltaic performance of quasi-solid-state DSSC with PEO₁₃BIm-I-based thixotropic gel electrolyte at different light intensities

Light intensity (mW cm^{-2})	V_{oc} (mV)	J_{sc} (mA cm^{-2})	FF	η (%)
100	733	10.71	0.67	5.25
67.8	713	7.44	0.69	3.67
55.1	707	6.05	0.70	2.98
42.2	699	4.61	0.70	2.27
19.6	668	2.28	0.70	1.06

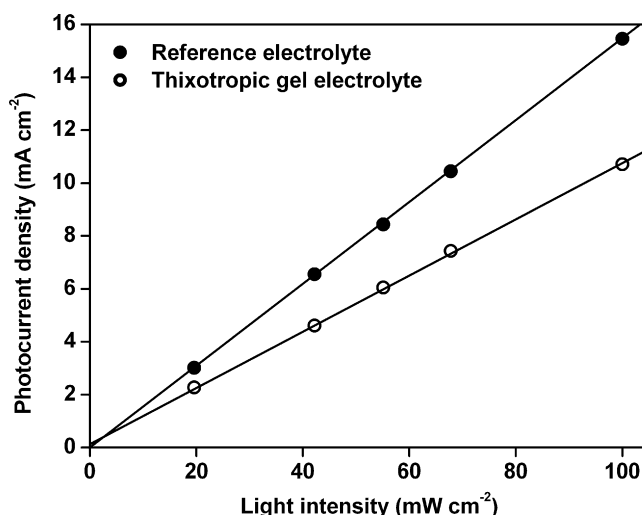


Fig. 5. Effect of light intensity on short-circuit current density of DSSCs with a reference liquid electrolyte (filled circle) and PEO₁₃BIm-I-based thixotropic gel electrolyte (open circle). The lines are extrapolated from J_{sc} data.

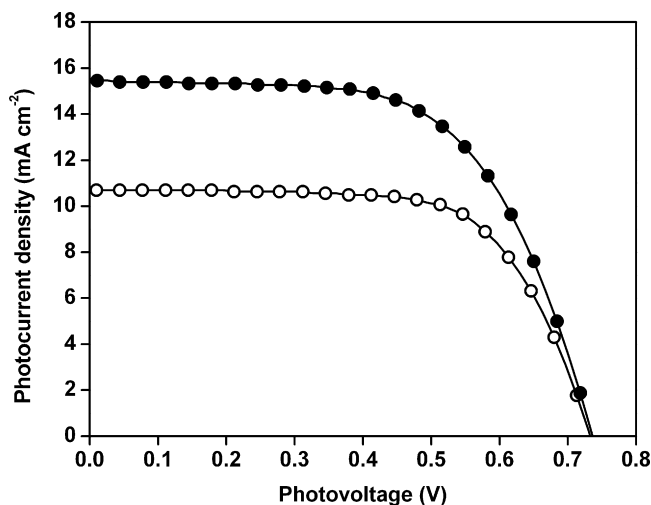


Fig. 6. Photocurrent density–voltage curves of DSSCs with a reference liquid electrolyte (filled circle: $V_{\text{oc}} = 736 \text{ mV}$; $J_{\text{sc}} = 15.45 \text{ mA cm}^{-2}$; FF=0.61; $\eta = 6.95\%$) and PEO₁₃BIm-I-based thixotropic gel electrolyte (open circle: $V_{\text{oc}} = 733 \text{ mV}$; $J_{\text{sc}} = 10.71 \text{ mA cm}^{-2}$; FF=0.67; $\eta = 5.25\%$): measured at AM 1.5 illumination (100 mW cm^{-2}); TiO₂ layer thickness of 11 μm .

cells were left on a laboratory shelf at room temperature and the conversion efficiency was found to be 94% of the original values after 6 months.

4. Conclusions

A novel thixotropic gel electrolyte employing a new type of ionic liquid, i.e., PEO-based bis-imidazolium diiodide salt, and hydrophilic silica nanoparticles is found to have many advantages in terms of its application in quasi-solid-state DSSCs. Upon incorporating the PEO units in a novel dicationic bis-imidazolium diiodide, thixotropic behaviour is clearly observed and the V_{oc} of the composite electrolyte can be improved significantly without using any electron scavenger. A DSSC with the PEO₁₃BIm-I-based thixotropic gel electrolyte yields good pho-

photovoltaic performance with $V_{oc} = 733$ mV, $J_{sc} = 10.71$ mA cm⁻². The FF is 0.67 and the η is 5.25% under AM 1.5 illumination (100 mW cm⁻²). These kinds of thixotropic gel electrolytes should be useful for assembling DSSCs without leakage and providing efficient photovoltaic output with long-term stability.

Acknowledgment

The authors gratefully acknowledge the financial support of the Korea Institute of Science and Technology (KIST) internal project under Contract No. 2E20010.

References

- [1] B. O'Regan, M. Grätzel, *Nature* 353 (1991) 737–740.
- [2] C.J. Barbe, F. Arendse, P. Comte, M. Jirousek, F. Lenzmann, V. Shklover, M. Grätzel, *J. Am. Ceram. Soc.* 80 (1997) 3157–3171.
- [3] M. Grätzel, *J. Photochem. Photobiol. A* 164 (2004) 3–14.
- [4] G. Smestad, C. Bignozzi, R. Argazzi, *Sol. Energy Mater. Sol. Cells* 32 (1994) 259–272.
- [5] Z.S. Wang, F.Y. Li, C.H. Huang, *J. Phys. Chem. B* 105 (2001) 9210–9217.
- [6] K. Hara, M. Kurashige, S. Ito, A. Shinpo, S. Suga, K. Sayama, H. Arakawa, *Chem. Commun.* (2003) 252–253.
- [7] L. Schmidt-Mende, U. Bach, R. Humphry-Baker, T. Horiuchi, H. Miura, S. Ito, S. Uchida, M. Grätzel, *Adv. Mater.* 17 (2005) 813–815.
- [8] M. Grätzel, *Nature* 414 (2001) 338–344.
- [9] Q. Wang, J.-E. Moser, M. Grätzel, *J. Phys. Chem. B* 109 (2005) 14945–14953.
- [10] N. Papageorgiou, Y. Athanassov, M. Armand, P. Bonhôte, H. Pettersson, A. Azam, M. Grätzel, *J. Electrochem. Soc.* 143 (1996) 3099–3108.
- [11] H. Matsumoto, T. Matsuda, T. Tsuda, R. Hagiwara, Y. Ito, Y. Miyazaki, *Chem. Lett.* 1 (2001) 26–27.
- [12] J. Dupont, R.F. De Souza, P.A.Z. Suarez, *Chem. Rev.* 102 (2002) 3667–3692.
- [13] P. Terech, R.G. Weiss, *Chem. Rev.* 97 (1997) 3133–3160.
- [14] W. Kubo, K. Murakoshi, T. Kitamura, S. Yoshida, M. Haruki, K. Hanabusa, H. Shirai, Y. Wada, S. Yanagida, *J. Phys. Chem. B* 105 (2001) 12809–12815.
- [15] N. Kimizuka, T. Nakashima, *Langmuir* 17 (2001) 6759–6761.
- [16] W. Kubo, T. Kitamura, K. Hanabusa, Y. Wada, S. Yanagida, *Chem. Commun.* (2002) 374–375.
- [17] E. Stathatos, P. Lianos, S.M. Zakeeruddin, P. Liska, M. Grätzel, *Chem. Mater.* 15 (2003) 1825–1829.
- [18] J.H. Kim, M.-S. Kang, Y.J. Kim, J. Won, N.-G. Park, Y.S. Kang, *Chem. Commun.* (2004) 1662–1663.
- [19] H. Usui, H. Matsui, N. Tanabe, S. Yanagida, *J. Photochem. Photobiol. A* 164 (2004) 97–101.
- [20] P. Wang, S.M. Zakeeruddin, P. Comte, I. Exnar, M. Grätzel, *J. Am. Chem. Soc.* 125 (2003) 1166–1167.
- [21] H. Yang, C. Yu, Q. Song, Y. Xia, F. Li, Z. Chen, X. Li, T. Yi, C. Huang, *Chem. Mater.* 18 (2006) 5173–5177.
- [22] S.Y. Huang, G. Schlichthorl, A.J. Nozik, M. Grätzel, A.J. Frank, *J. Phys. Chem. B* 101 (1997) 2576–2582.
- [23] P. Wang, S.M. Zakeeruddin, J.E. Moser, M.K. Nazeeruddin, T. Sekiguchi, M. Grätzel, *Nat. Mater.* 2 (2003) 402–407.
- [24] M.K. Nazeeruddin, A. Kay, I. Rodicio, R. Humphry-Baker, E. Müller, P. Liska, N. Vlachopoulos, M. Grätzel, *J. Am. Chem. Soc.* 115 (1993) 6382–6390.
- [25] A.F. Bückmann, M. Morr, G. Johansson, *Makromol. Chem.* 182 (1981) 1379–1384.
- [26] R. Komiya, L. Han, R. Yamanaka, A. Islam, T. Mitate, *J. Photochem. Photobiol. A* 164 (2004) 123–127.